Materials Advances

ROYAL SOCIETY OF CHEMISTRY

PAPER

View Article Online
View Journal | View Issue

Cite this: *Mater. Adv.*, 2022, 3, 5012

Nitro-based and nitro-free tri-cationic azole salts: a unique class of energetic green tri-ionic salts obtained from the reaction with nitrogen-rich bases†

Ajay Kumar Chinnam, [a] Richard J. Staples, [b] Gang Zhao [a] and Jean'ne M. Shreeve *[a]

Nitrogen-rich heterocycles are essential for designing novel energetic green materials with the combination of high explosive performance and acceptable mechanical sensitivities. In this work, two sets of high nitrogen-azoles, derived from tetrazoles and triazole assemblies with *N*-trinitromethane, 5,5′-(2-(trinitromethyl)-2*H*-1,2,3-triazole-4,5-diyl)bis(1*H*-tetrazole) (TBTN) and *N*-methylene tetrazole, 5,5′-(2-((1*H*-tetrazol-5-yl)methyl)-2*H*-1,2,3-triazole-4,5-diyl)bis(1*H*-tetrazole) (TBTT) are described. Their molecular structures were confirmed using multinuclear (^{1}H, ^{13}C, and ^{15}N) NMR spectra and single-crystal X-ray diffraction analysis. These molecules are attention attracting results emanating from methodologies utilized to access a unique class of tri-ionic salts in reaction with nitrogen-rich bases. The thermostabilities, mechanical sensitivities, and detonation properties of all new compounds were determined. Surprisingly, the nitro-based tri-cationic salts, **5b** (Dv = 9376 m s^{-1}) and **5c** (Dv = 9418 m s^{-1}), have excellent detonation velocities relative to **HMX** (Dv = 9144 m s^{-1}), while those of the nitro-free tri-cationic salts, **8b·H$_2$O** (Dv = 8998 m s^{-1}) and **8c·0.5H$_2$O** (Dv = 9058 m s^{-1}), are superior to that of **RDX** (Dv = 8795 m s^{-1}) and approach HMX values. Additionally, nearly all new compounds are insensitive to mechanical stimuli because of the high percentage of hydrogen bond interactions (HBs) between the anions and cations, which are evaluated using two-dimensional (2D) fingerprint and Hirshfeld surface analyses. It is believed that the work presented here is the first example of high-performing and insensitive tri-cationic energetic salts, which may establish a discovery platform for the "green" synthesis of future energetic materials.

Received 9th April 2022,
Accepted 9th May 2022

DOI: 10.1039/d2ma00406b

rsc.li/materials-advances

Introduction

The serious global health problem with the world's most widely used high energy dense materials, such as TNT (trinitrotoluene), RDX (1,3,5-trinitroperhydro-1,3,5-triazine), HMX (1,3,5,7-tetranitro-1,3,5,7-tetrazocane), and lead azide (LA), is primarily environmental which gives rise to a particular need for action to find alternatives.[1] In the past two decades, nitrogen-rich heterocycles have received considerable attention in the design and synthesis of high energy density materials (HEDMs) while attempting to balance between high detonation performance, sensitivity, and environmental concerns.[2,3] In general, five-membered ring heterocycles (tetrazole, triazole, pyrazole, furazan, *etc.*) have been widely used in developing various high-performing nitrogen-rich frameworks.[4–7] Among them, triazoles, and tetrazoles have attracted particular interest due to their high densities and high heats of formation, which are very important in the detonation performance of the resulting materials.[8,9] Several synthetic methodologies have been developed by combining mixed azole frameworks and explosophores such as nitro (–NO$_2$),[10,11] nitramine (–NHNO$_2$),[12] dinitromethane (–C(NO$_2$)$_2$),[13,14] and trinitromethane (–C(NO$_2$)$_3$),[15–17] which enhance the density and detonation performance. However, the main drawback of such molecules is that they are less thermally stable and very sensitive (high impact and friction sensitivities).

Various methods have been developed to enhance the thermostability and improve sensitivity by synthesizing salts through neutralization or metathesis reactions with various protonated cations or co-crystallization with a less sensitive material.[18–21] The advantages of energetic salts include lower vapor pressure, larger positive heats of formation, higher thermostability, and lower sensitivity. Ammonium-based cations are

[a] *Department of Chemistry, University of Idaho, Moscow, Idaho, 83844-2343, USA. E-mail: jshreeve@uidaho.edu*
[b] *Department of Chemistry, Michigan State University East Lansing, MI, 48824, USA*

† Electronic supplementary information (ESI) available. CCDC 2160564–2160567. For ESI and crystallographic data in CIF or other electronic format see DOI: https://doi.org/10.1039/d2ma00406b

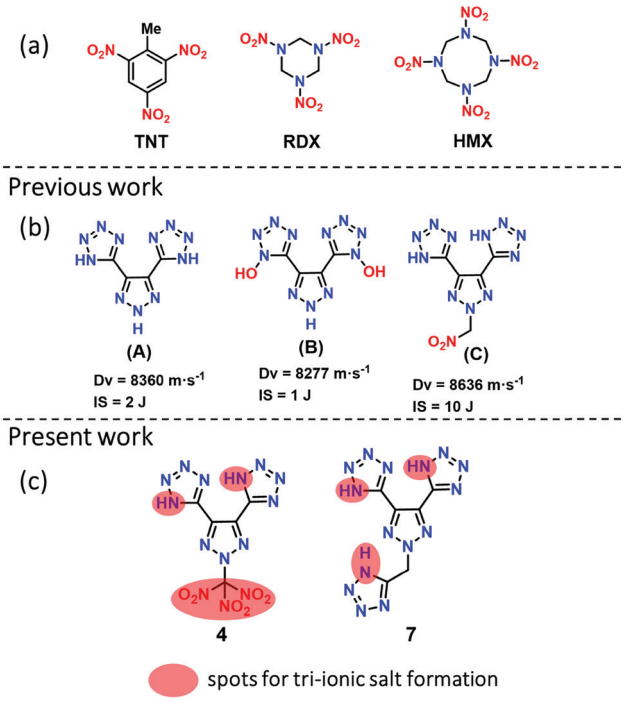

Fig. 1 (a) Energetic materials, TNT, RDX, and HMX; (b) examples of nitrogen-rich green energetic materials; (c) and new molecules; red circle for accessing anions.

essential in preparing energetic salts, frequently helping hydrogen bond (HB) formation with the corresponding anions.[22,23] There are several energetic salts based on mono- and di-cationic salts. Not surprisingly, the latter shows higher detonation performances than mono-cationic salts.[24] Also, it is often crucial to select a suitable anion such as one which is nitro-based for the preparation of high performing energetic salts. However, there are only few studies have focused on nitro-free anions based on nitrogen-rich anions or N-oxides in recent years,[25,26] for instance, compounds **A** and **B**, which form di-cationic salts by a double deprotonation of tetrazole NH or *N*-hydroxide (Fig. 1).[27] Compounds **A** and **B** are examples of energetic green materials with excellent positive heats of formation of 801.0 kJ mol^{-1} and 823 kJ mol^{-1}, respectively. These derivatives have outstanding thermostabilities (>240 °C) but are highly sensitive to impact (<3 J), which makes handling them a challenge in practical applications.

Very recently, our group reported compound **C** with improved detonation properties and low sensitivity to impact by introducing a nitro-methyl group on the nitrogen scaffold of **A**.[28] Although compound **C** meets the required sensitivity properties, the detonation properties are still relatively low compared with those of RDX. Because of our interest in the development of novel high performing, eco-friendly insensitive materials, we now report two sets of nitrogen-rich materials, based on the skeleton of compound **A**. These compounds contain the high performing explosophore, trinitromethane ($-C(NO_2)_3$) (**4**), and the nitrogen-rich stable and insensitive *N*-methylene-tetrazole (**7**). Compounds **4** and **7** are unusual with an advantage for preparing tri-cationic salts by neutralizing them with bases. All compounds are isolated in excellent yields and thoroughly characterized by advanced spectroscopy. The structures of **4**, **5a**, **5b**, and **7** were analyzed by using single-crystal X-ray diffraction methods. Most of the compounds are highly thermostable and insensitive to impact and friction. All new compounds have high nitrogen–oxygen content (73.15 to 82.47%), which results in high positive heats of formation and detonation performances. Most new compounds have higher detonation properties than RDX, while the tri-cationic salts, **5b** and **5c**, have a superior performance relative to HMX. Furthermore, the syntheses of high nitrogen-rich derivative **7** and its energetic salts are achieved under "green reaction conditions," which are highly desirable for the synthesis of future energetic materials.

Results and discussion

Synthesis

The preparation of potassium 4,5-dicyano-1,2,3-triazol-2-ide, **1**, was adapted from a previously reported procedure through the reaction of diaminomaleonitrile with sodium nitrite and subsequent reaction with one equivalent of potassium hydroxide.[29] Then **1** was treated with chloroacetone under acetonitrile reflux resulting in 2-(2-oxopropyl)-2*H*-1,2,3-triazole-4,5-dicarbonitrile, **2**, in 88% yield (Scheme 1). Having the two functional groups on **2** allowed the selection of suitable reagents and reaction conditions to achieve our first target compound, **4**. First, both nitriles reacted with sodium azide in the presence of a zinc chloride catalyst in an aqueous solution at reflux temperature to obtain bis tetrazole (**3**) in excellent yields without the involvement of *N*-acetone. Later, the nitration of **3** using mixed acids at 0 °C gave a colorless solid of 5,5′-(2-(trinitromethyl)-2*H*-1,2,3-triazole-4,5-diyl)bis(1*H*-tetrazole), **4**, in 95% yield. A series of bases, *viz.*, ammonia, hydroxylamine, and hydrazine were reacted with **4** at room temperature to give the energetic salts, **5a–c**, in 80–98% yields (Scheme 1). The reaction of **4** with aqueous ammonia or anhydrous ammonia in protonated solvents such as in methanol or ethanol gave only the di-cationic salt **5a**, and no product was formed in acetonitrile. Surprisingly, tri-cationic salts with hydroxylammonium (**5b**), hydrazinium (**5c**), and anions were obtained as yellow solids when acetonitrile was the solvent.

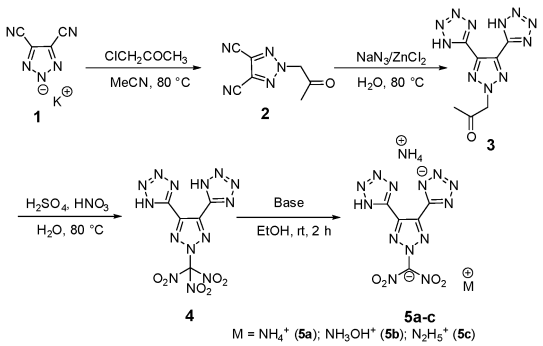

Scheme 1 Synthesis of nitrogen-rich energetic salts **5a–c**.

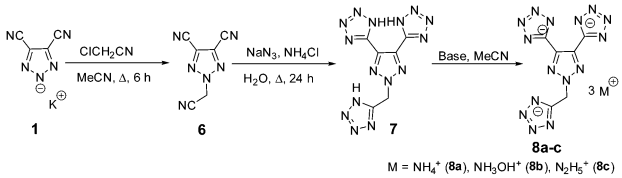

Scheme 2 Synthesis of nitrogen-rich energetic salts **8a–c**.

Next nitro-free heterocycles were investigated by incorporating additional tetrazole rings on the triazole ring and neutralizing them with nitrogen-rich bases. Not surprisingly, N-substituted acetonitrile, **6,** was obtained in various yields from the reaction of potassium salt, **1**, with chloroacetonitrile in acetonitrile under reflux conditions (Scheme 2). With the trinitrile derivative **6** in hand, it was reacted with sodium azide using zinc chloride as a catalyst in an aqueous solution at reflux temperature to give a complex metal salt mixture, from which it was not possible to isolate pure **7**. However, under mildly acidic conditions, with ammonium chloride as a catalyst, tri-tetrazole, **7**, was formed in a high yield. Then, the three tetrazole rings of **7** were neutralized with aqueous bases, ammonia, hydroxylamine, and hydrazine, in acetonitrile to obtain nitrogen-rich tri-ionic salts **8a–c** (Scheme 2).

^{15}N NMR spectroscopy

Since these new compounds have a high nitrogen content (>70%), ^{15}N NMR spectra of two sets were recorded and compared (Fig. 2 and 3). In the first set, the ^{15}N NMR spectra of nitro group-based compound **4** and its hydrazinium salt, **5c**, were recorded in DMSO-d_6 (Fig. 2). There are five signals in the ^{15}N NMR spectrum of **4** due to two-fold rotational symmetry. The signal for trinitromethane was observed at $\delta = -40.3$ (N1) followed by triazole ring nitrogen signals at $\delta = -150.5$ (N5) and $\delta = -22.0$ (N3) and the tetrazole ring nitrogen signals at $\delta = -79.4$ (N4) and $\delta = -45.1$ (N5). In the trihydrazinium cationic salt, **5c**, there are six signals, the hydrazinium nitrogen atom at high field $\delta = -330.6$ (N6), while the azole ring nitrogen signals of the anion were observed from $\delta = -7.7$ to -139.1. They are significantly different from those of neutral compound **4**. In addition, there is a signal for the dinitro methane nitrogen

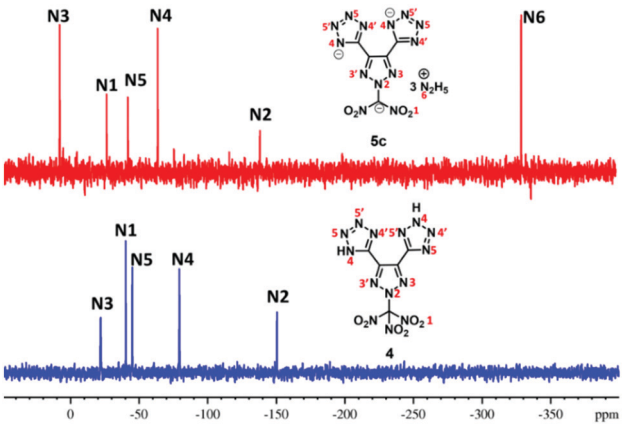

Fig. 2 ^{15}N NMR spectra of **4** and **5c**.

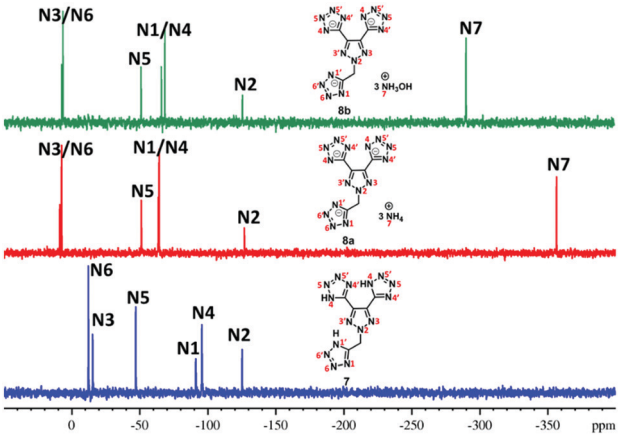

Fig. 3 ^{15}N NMR spectra of **7**, **8a** and **8b**.

at $\delta = -26.7$ (N1), two signals for the triazole nitrogen atoms at $\delta = -139.1$ (N2) and $\delta = -7.7$ (N3), and two nitrogen signals for the tetrazole anion at $\delta = -64.2$ (N4) and $\delta = -42.3$ (N5).

The ^{15}N NMR spectra of the nitro free energetic compound, **7**, and its salts, **8a** and **8b,** in DMSO-d_6 (Fig. 3) are similar to that of compound **4**. One drop of D_2O was added to compound **7** in order to control the proton exchange on the triazole rings. There are three tetrazole rings in compound **7** bonded to the triazole ring: two of them through a C–C bond, while the third *via* a *N*-methylene bridge. Since the molecular structure of **7** has *C*2-symmetry, six signals are found in the ^{15}N NMR spectrum. The triazole ring atom signals were observed at $\delta = -125.5$ (N2) and $\delta = -15.5$ (N3), while the tetrazole ring resonances were observed between $\delta = -12.3$ and -95.8. In the ^{15}N NMR of both salts, **8a** and **8b**, seven signals were observed because of the tri-tetrazole anion framework (six signals) and cation (one signal). The signals for the corresponding cation of 8a (NH_4^+) are observed at $\delta = -356.6$ (N7) and **8b** (NH_4OH^+) at $\delta = -290.8$ (N7). The nitrogen signals for the anion were found between $\delta = 8.3$ and -127.1 (for **8a**) and $\delta = 7.2$ and -126.0 (for **8b**), which are significantly different from those of the parent compound **7**.

Single crystal X-ray analysis

Compound **4** was crystallized in a saturated methanol solution by slow evaporation at room temperature. The crystals of **4** were obtained with one molecule of methanol in the crystal structure. It crystallizes in the monoclinic space group $P2_1/c$ ($Z = 4$) with a calculated density of 1.832 g cm^{-3} at 100 K. As is shown in Fig. 4a, there are two tetrazole rings in two different isomers due to the position of NH. The molecular structure is arranged in a twofold screw axis with a glide plane through the center of the molecule. The bond lengths and angles within the 1,2,3-triazole and tetrazole rings are between typical C–N, N–N, and C–C single and double bonds. The C1–C2 bond length in 1,2,3-triazole is 1.4218 (18) Å, which is slightly shorter in comparison to the C–C bond between typical 1,2,3-triazole and tetrazole rings (1.4569 (18) Å and 1.4595 (17) Å). The N2–C5 bond length of the *N*-trinitromethane carbon is 1.4096 (16) Å, which is

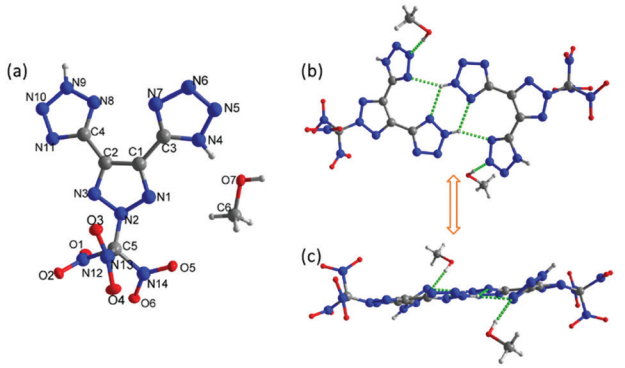

Fig. 4 (a) Thermal ellipsoid plot (50%) and labeling scheme for **4·MeOH**. (b and c) HB system connects two molecules of **4·MeOH**.

relatively shorter than the N–C bond of trinitromethane (between the range of 1.5325–1.5565 Å). In the crystal packing structure of **4·MeOH**, there are two pairs of hydrogen bonds between the NH of one of the tetrazoles and the tetrazole ring of the adjacent molecule. In contrast, the NH of the second tetrazole participates in hydrogen bonding with the cosolvent methanol (Fig. 4b and c).

The mono hydrated diammonium salt of **5a·H$_2$O** was obtained by slow evaporation in a mixture of water and methanol. It belongs to the monoclinic space group *I*2/*a* (*Z* = 8) with a calculated density of 1.753 g cm^{-3} at 99.99 K (Fig. 5a). Only one tetrazole molecule is deprotonated to form a tetrazole anion and eliminate one nitro group to form the dinitromethane anion, which is neutralized with two ammonium ions. Dianionic nitrogen-rich skeleton is neutralized with two ammonium ions. The anion ring system is nearly planar with torsion angles of C4–C2–C1–C4 = −5.0°(3), C2–C1–C4–N11 = −3.8°(3), and C1–C2–C3–N7 = 0.5°(3) and the two nitro groups together with the atom C5 form another plane. The angle between the two planes is 75.97°. The N–C bond lengths of N–C(NO$_2$)$_2$ and –C(NO$_2$)$_2$ are slightly lower than those in the molecular structure of **4·MeOH**. There are several hydrogen bonds (N–H···N and N–H···O) which are observed in the three-dimensional packing network (Fig. 5b).

Crystals of the hydroxylammonium salt, **5b,** were obtained with one water molecule from the mixture of ethanol and water.

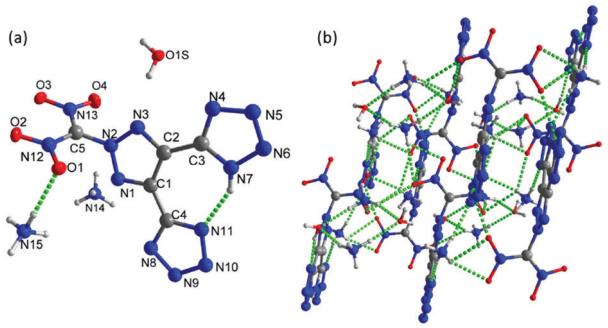

Fig. 5 (a) Thermal ellipsoid plot (50%) and labeling scheme for **5a·H$_2$O**. (b) A *b* axis view of the ball-and-stick packing diagram of **5a·H$_2$O**.

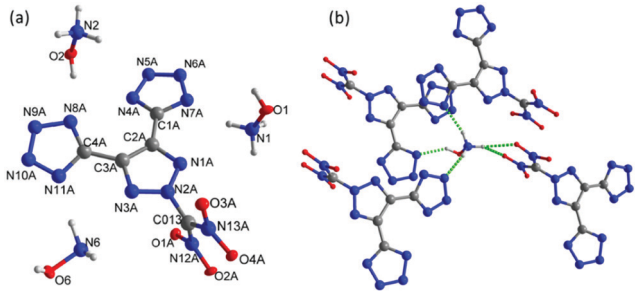

Fig. 6 (a) Thermal ellipsoid plot (50%) and labeling scheme for **5b·H$_2$O**. (b) Hydrogen bonding interaction between hydroxylammonium cations and anions in the crystal structure of **5b·H$_2$O**.

The water molecule and one of the hydroxylammonium cations are found to have a disorder, which is removed for clarity (Fig. 6a). **5b·H$_2$O** crystallizes in the monoclinic space group *Ia* (*Z* = 8) with a crystal density of 1.759 g cm^{-3} at 100 K. Unlike **5a·H$_2$O**, both tetrazole rings were deprotonated and eliminated along with one nitro group to form a tri-anionic fragment, which coordinates with three hydroxylammonium ions. The tri-anionic structure is arranged very much like the molecular structure of **4·MeOH** (with a twofold screw axis). All the atoms of the 1,2,3-triazole are coplanar while the dinitro methane group is found on the perpendicular plane at an angle of 85.59°. The bond lengths in the triazole and tetrazole rings are between typical single and double bonds. The N–C bond lengths of N–C(NO$_2$)$_2$ and –C(NO$_2$)$_2$ are nearly identical to those in the molecular structure of **5a**. In the crystal packing of compound **5b·H$_2$O**, there are many strong intermolecular hydrogen bond interactions due to the hydroxylamine groups, nitro oxygen atoms, and nitrogen atoms in both the anions and cations (Fig. 6b).

Crystals of 7 were obtained without water or solvent molecule from the mixture of acetonitrile and hydrochloric acid and crystallized in the monoclinic space group $P2_1/c$ (*Z* = 4) with a crystal density of 1.772 g cm^{-3} at 100 K and a twofold axis passing through the center of the molecule (Fig. 7a). The bond lengths and angles within the azole rings are within the range of normal C–N, N–N, and C–C single and double bonds. The dihedral angle between the mean planes through the 1,2,3-triazole and *N*-methylene bridge tetrazole rings was found to be

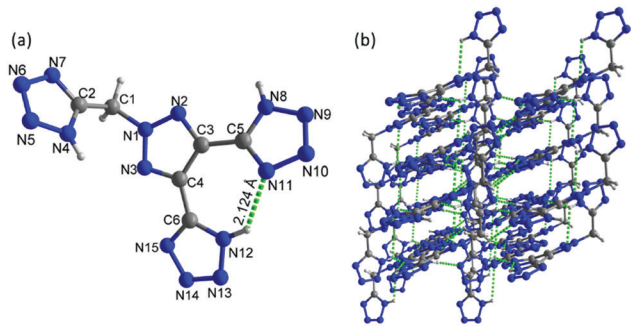

Fig. 7 (a) Thermal ellipsoid plot (50%) and labeling scheme for **7**. (b) A *b* axis view of the ball-and-stick packing diagram of **7**.

Table 1 Energetic properties and detonation parameters

Comp.	T_d[a] [°C]	ρ[b] [g cm^{-3}]	ΔH_f[c] [kJ mol^{-1}]/[kJ g^{-1}]	V_D[d] [m s^{-1}]	P[e] [GPa]	IS[f] [J]	FS[g] [N]	N + O[h] [%]
4	157	1.84	982.4/2.77	9101	35.93	9	120	82.47
5a·H$_2$O	146	1.71	251.4/0.69	8176	24.78	>60	>360	80.30
5b	196	1.76	1399.3/3.42	9376	37.25	38	360	82.32
5c	169	1.74	1500.7/3.70	9418	34.68	35	360	81.45
7	284	1.75	1228.8/4.27	8362	26.14	55	>360	73.15
8a·H$_2$O	256	1.57	1559.4/4.37	8598	26.11	>60	>360	75.25
8b·H$_2$O	245	1.64	1637.2/4.05	8998	30.74	>60	>360	78.42
8c·0.5H$_2$O	265	1.63	1858.6/4.73	9058	29.43	>60	>360	77.14
A[i]	277	1.69	823.0/3.46	8360	26.00	2	240	78.46
B[i]	246	1.67	801.0/3.90	8277	24.80	1	240	75.11
C[j]	281	1.79	945.8/3.35	8636	29.50	10	240	76.58
RDX[k]	204	1.80	70.7/0.32	8795	34.90	7.5	120	81.06
HMX[k]	280	1.90	74.8/0.25	9144	39.20	7.4	120	81.06

[a] Decomposition temperature (onset). [b] Density measured by a gas pycnometer at 25 °C. [c] Calculated molar enthalpy of formation. [d] Calculated detonation velocity. [e] Calculated detonation pressure. [f] Impact sensitivity. [g] Friction sensitivity. [h] Combined nitrogen and oxygen content. [i] Ref. 24. [j] Ref. 25. [k] Ref. 3.

67.83°. In the crystal packing diagram, there are several inter- and intramolecular bonds (N–H···N), which form a three-dimensional framework (Fig. 7b).

Physicochemical properties

Thermostabilities and physicochemical properties of all new compounds were investigated and are compared with those of high performing materials such as RDX and HMX in Table 1. The density of all new compounds was measured using a helium gas pycnometer at 25 °C. All new compounds were confirmed by elemental analysis prior to measuring densities which are found between 1.57 and 1.84 g cm^{-3}. Due to the presence of the trinitromethyl group, compound **4** has the highest density at 1.84 g cm^{-3}, while those of other compounds, such as the poly nitrogen compound, **7** (1.75 g cm^{-3}), and dinitromethane salts, **5b** (1.76 g cm^{-3}) and **5c** (1.74 g cm^{-3}), approach that of RDX (1.80 g cm^{-3}) (Fig. 8a). Thermostabilities of all the new compounds were measured using differential scanning calorimetry at a heating rate of 5 °C per minute and were found to have excellent values ranging from 157–284 °C. Nitro compounds, **4**, **5a–c**, and the tritetrazole compound, **7**, decomposed without melting, while the hydrated salts **8a–c** melted prior to decomposing in the range of 245–265 °C. The heat of formation calculations for all the new compounds were carried out using the Gaussian 03 (Revision E.01) suite of programs.[30] Having the advantage of a poly nitrogen-rich azole backbone and trications, all new compounds have a high positive enthalpy of formation with values ranging from 0.69 to 4.53 kJ g^{-1}, which are greater than those of RDX (0.36 kJ g^{-1}) and HMX (0.25 kJ g^{-1}) (Fig. 8a).

Using the experimental density and calculated heats of formation, detonation properties were obtained using the EXPLO5 (Version 6.01) computer code.[31] Because of high densities and positive heats of formation, detonation velocities (V_D) and detonation pressures (P) of the new energetic compounds have excellent performance. Except for the polytetrazole compound, **7** (8362 m s^{-1}), ammonium salt, **8a** (8176 m s^{-1}), and ammonium salts, **5a·H$_2$O** (8176 m s^{-1}), all other compounds especially, the nitro free energetic salts, **8b·H$_2$O** (8998 m s^{-1}) and **8c·0.5H$_2$O** (9058 m s^{-1}), display outstanding performances compared with RDX (8795 m s^{-1}). Among all these compounds, the detonation properties of the trinitro compound, **4** (9101 m s^{-1}), and its tricationic salts, **5b** (9376 m s^{-1}) and **5c** (9418 m s^{-1}), are superior to those of HMX (9144 m s^{-1}) (Fig. 8b).

The impact sensitivity experiments were measured according to STANAG 4489 using a BAM drop hammer for the safety and handling of these new materials.[32,33] The friction sensitivity experiments were measured according to STANAG 4487 using a BAM friction tester (Fig. 9).[34] The trinitromethane compound **4**, is sensitive to mechanical stimuli (impact sensitivity (IS) = 9 J; friction sensitivity (FS) = 120 N), while the other

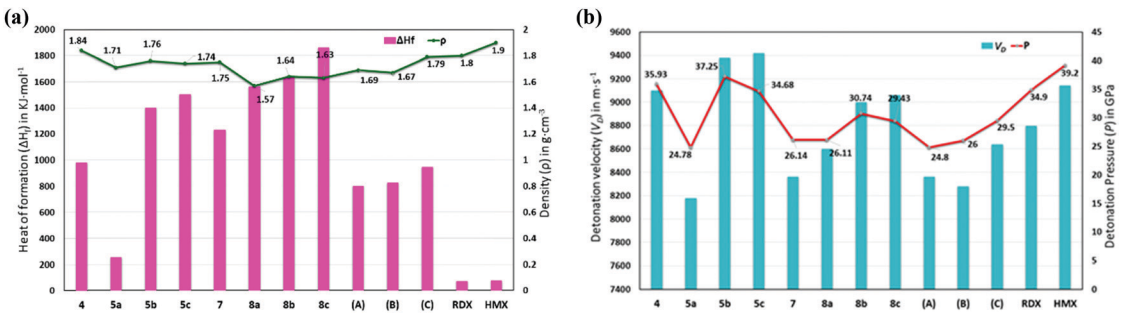

Fig. 8 Calculated heats of formation, experimental densities (a), calculated detonation velocities, and detonation pressures (b) of **4**, **5a–c**, **7**, **8a–c**, and compared with those of **A**, **B**, **C**, **RDX**, and **HMX**.

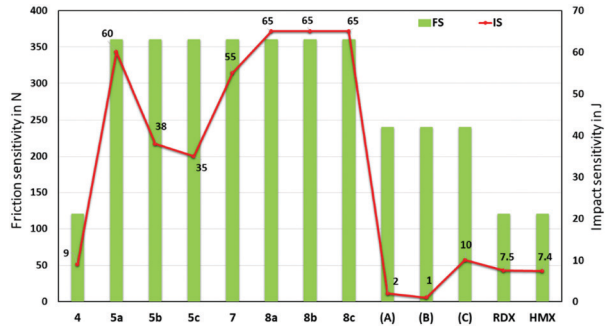

Fig. 9 Experimental impact and friction sensitivity of **4**, **5a–c**, **7**, **8a–c**, and compared with those of reference compounds, **A**, **B**, **C**, **RDX**, and **HMX**.

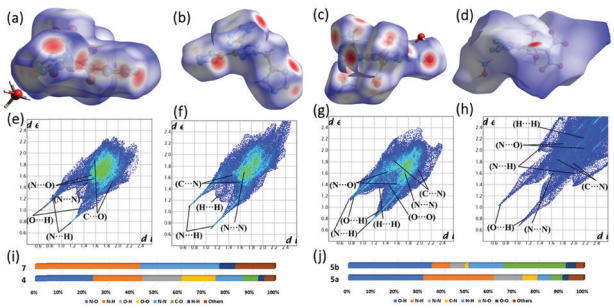

Fig. 10 Hirshfeld surface calculations (a–d), and 2D fingerprint plots (e–h) of the crystal structures **4**, **7**, **5a·H$_2$O**, and **5b·H$_2$O**. Populations of individual contacts for **4·MeOH**, **7** (i), and **5a·H$_2$O**, **5b·H$_2$O** (j).

new compounds are much less sensitive (IS = 35–65 J; FS = 360 N). Most importantly, the high performing tri-cationic salts, **5b** (IS = 38 J; FS = 360 N), **5c** (IS = 35 J; FS = 360 N), **8b·H$_2$O** (IS = 65 J; FS > 360 N), and **8b·0.5H$_2$O** (IS = 65 J; FS > 360 N), have better mechanical stabilities than the high energy explosives, **RDX** (IS = 7.5 J; FS = 120 N) and **HMX** (IS = 7.4 J; FS = 120 N).

The Hirshfeld electrostatic surfaces and two-dimensional (2D) fingerprint of the crystals were used to understand the inert- and intramolecular interactions (Fig. 10).[35] In the Hirshfeld surface analysis, red dots indicate the close contact intermolecular hydrogen bonds (HBs). The blue area is the O–C, C–C, and C–N interactions, which tell the high energy and sensitivity features of an energetic material. In Fig. 10e–h, 2D fingerprint plots, the spikes indicate the strong O···H and N···H hydrogen bonding interactions. Based on the crystal structures, **5a** has large O···H (31.9%) and N···H (30.0%) interactions, while these HB interactions decreased in **7** (N···H, 43.9%), **5b** (O···H, 35.6%; N···H, 7.8%), and **4** (O···H, 16.4%; N···H, 20.7%), respectively. As a result of the HB-interactions, compounds **5a**, **5b**, and **7** are more stable and less sensitive than compound **4**, which are comparable with experimental results (Fig. 10).

Conclusions

In summary, we have described two sets of novel nitrogen-rich materials based on 4,5-bis(tetrazol-5-yl)-1,2,3-triazole. This is the first report of high-performing and insensitive tri-cationic energetic salts. The synthesis and energetic properties of these compounds focus on two crucial components which are in high demand in the development of high performing, insensitivity, and eco-friendly novel energetic materials. Synthesis of these compounds is achieved in five to six synthetic steps in essentially quantitative yields. In particular, the nitro-group free energetic azole, **7**, and its tri-ionic salts are obtained under "green reaction conditions". All these compounds were fully characterized by multinuclear (^{1}H, ^{13}C, and ^{15}N) NMR, FTIR spectroscopy, and elemental analysis. The structures of compounds **4**, **5a·H$_2$O**, **5b**, and **7** were determined by single-crystal X-ray diffraction. After confirming these crystal structures, the stability and sensitivity properties are predicted using Hirshfeld surfaces and 2D fingerprint analysis and compared with experimental thermostabilities and mechanical sensitivities where the agreement is satisfactory. Furthermore, the enthalpy of formation and energetic properties of all new compounds were calculated. Most new tri-ionic salts have excellent energetic performances compared with nitramine-based high-energy density materials, RDX and HMX. Moreover, this study is expected to provide a potential guide for the "green" synthesis of nitrogen-rich materials with fine-tuning properties of high energy and acceptable sensitivity for future energetic applications.

Data availability

Details of experimental details, theoretical calculations, X-ray crystal diffraction data and crystal structures for compounds **4·MeOH**, **5a·H$_2$O**, **5b·H$_2$O**, and **7**, and NMR spectra are provided in the ESI.†

Author contributions

A. K. C. and G. Z.: investigation, methodology, and initial characterization of this work. R. J. S.: X-ray data collection and solving the structures. A. K. C. and J. M. S.: conceptualisation, manuscript writing – review and editing, and supervision.

Conflicts of interest

There are no conflicts to declare.

Acknowledgements

The Rigaku Synergy S Diffractometer was purchased with support from the National Science Foundation MRI program under Grant No. 1919565.

Notes and references

1 T. Brinck, *Green Energetic Materials*, Wiley: Hoboken, NJ, 2014.
2 T. M. Klapötke, P. C. Schmid, S. Schnell and J. Stierstorfer, *Chem. – Eur. J.*, 2015, **21**, 9219–9228.

3 R. Meyer, J. Köhler and A. Homburg, *Explosives*, John Wiley & Sons, 2016.
4 M. N. Glukhovtsev, H. Jiao and P. R. Schleyer, *Inorg. Chem.*, 1996, **35**, 7124–7133.
5 J. C. Gálvez-Ruiz, G. Holl, K. Karaghiosoff, T. M. Klapötke, K. Löhnwitz, P. Mayer, H. Nöth, K. Polborn, C. J. Rohbogner, M. Suter and J. J. Weigand, *Inorg. Chem.*, 2005, **44**, 4237–4253.
6 P. Yin, C. He and J. M. Shreeve, *J. Mater. Chem. A*, 2016, **4**, 1514–1519.
7 Q. Yu, A. K. Chinnam, P. Yin, G. H. Imler, D. A. Parrish and J. M. Shreeve, *J. Mater. Chem. A*, 2020, **8**, 5859–5864.
8 A. A. Dippold, D. Izsak and T. M. Klapötke, *Chem. – Eur. J.*, 2013, **19**, 12042–12051.
9 H. Xue, Y. Gao, B. Twamley and J. M. Shreeve, *Chem. Mater.*, 2005, **17**, 191–198.
10 D. Fischer, J. L. Gottfried, T. M. Klapötke, K. Karaghiosoff, J. Stierstorfer and T. G. Witkowski, *Angew. Chem., Int. Ed.*, 2016, **55**, 16132–16135.
11 P. Yin, J. Zhang, G. H. Imler, D. A. Parrish and J. M. Shreeve, *Angew. Chem., Int. Ed.*, 2017, **56**, 8834–8838.
12 H. Wei, C. He, J. Zhang and J. M. Shreeve, *Angew. Chem., Int. Ed.*, 2015, **54**, 9367–9371.
13 Y. Zhou, H. Gao and J. M. Shreeve, *Energy Mater. Front.*, 2020, **1**, 2–15.
14 S. Dharavath, J. Zhang, G. H. Imler, D. A. Parrish and J. M. Shreeve, *J. Mater. Chem. A*, 2017, **5**, 4785–4790.
15 G. Zhao, D. Kumar, P. Yin, C. He, G. H. Imler, D. A. Parrish and J. M. Shreeve, *Org. Lett.*, 2019, **21**, 1073–1077.
16 Q. Yu, P. Yin, J. Zhang, C. He, G. H. Imler, D. A. Parrish and J. M. Shreeve, *J. Am. Chem. Soc.*, 2017, **139**, 8816–8819.
17 G. Zhao, P. Yin, D. Kumar, G. H. Imler, D. A. Parrish and J. M. Shreeve, *J. Am. Chem. Soc.*, 2019, **141**, 19581–19584.
18 H. Gao and J. M. Shreeve, *Chem. Rev.*, 2011, **111**, 7377–7436.
19 D. Srinivas, V. D. Ghule, K. Muralidharan and H. D.-B. Jenkins, *Chem. – Asian J.*, 2013, **8**, 1023–1028.
20 T. G. Witkowski, E. Sebastiao, B. Gabidullin, A. Hu, F. Zhang and M. Murugesu, *ACS Appl. Energy Mater.*, 2018, **1**, 589–593.
21 J. C. Bennion and A. J. Matzger, *Acc. Chem. Res.*, 2021, **54**, 1699–1710.
22 J. H. Zhang, Q. H. Zhang, T. T. Vo, D. A. Parrish and J. M. Shreeve, *J. Am. Chem. Soc.*, 2015, **137**, 1697–1704.
23 R. Bu, Y. Xiong, X. Wei, H. Li and C. Zhang, *Cryst. Growth Des.*, 2019, **19**, 5981–5997.
24 J. Zhang, S. Dharavath, L. A. Mitchell, D. A. Parrish and J. M. Shreeve, *J. Am. Chem. Soc.*, 2016, **138**, 7500–7503.
25 A. A. Dippold and T. M. Klapötke, *J. Am. Chem. Soc.*, 2013, **135**, 9931–9938.
26 D. Fischer, T. M. Klapötke, D. G. Piercey and J. Stierstorfer, *Chem. – Eur. J.*, 2013, **19**, 4602–4613.
27 A. A. Dippold, D. Izsak, T. M. Klapötke and C. Pflueger, *Chem. – Eur. J.*, 2016, **22**, 1768–1778.
28 G. Zhao, C. He, H. Gao, G. H. Imler, D. A. Parrish and J. M. Shreeve, *New J. Chem.*, 2018, **42**, 16162–16166.
29 C. M. Sabaté, E. Jeanneau and H. Delalua, *Dalton Trans.*, 2012, **41**, 3817–3825.
30 M. J. Frisch, G. W. Trucks, H. B. Schlegel, G. E. Scuseria, M. A. Robb, J. R. Cheeseman, J. A. Montgomery Jr., T. Vreven, K. N. Kudin, J. C. Burant, J. M. Millam, S. S. Iyengar, J. Tomasi, V. Barone, B. Mennucci, M. Cossi, G. Scalmani, N. Rega, G. A. Petersson, H. Nakatsuji, M. Hada, M. Ehara, K. Toyota, R. Fukuda, J. Hasegawa, M. Ishida, T. Nakajima, Y. Honda, O. Kitao, H. Nakai, M. Klene, X. Li, J. E. Knox, H. P. Hratchian, J. B. Cross, V. Bakken, C. Adamo, J. Jaramillo, R. Gomperts, R. E. Stratmann, O. Yazyev, A. J. Austin, R. Cammi, C. Pomelli, J. W. Ochterski, P. Y. Ayala, K. Morokuma, G. A. Voth, P. Salvador, J. J. Dannenberg, V. G. Zakrzewski, S. Dapprich, A. D. Daniels, M. C. Strain, O. Farkas, D. K. Malick, A. D. Rabuck, K. Raghavachari, J. B. Foresman, J. V. Ortiz, Q. Cui, A. G. Baboul, S. Clifford, J. Cioslowski, B. B. Stefanov, G. Liu, A. Liashenko, P. Piskorz, I. Komaromi, R. L. Martin, D. J. Fox, T. Keith, M. A. Al-Laham, C. Y. Peng, A. Nanayakkara, M. Challacombe, P. M. W. Gill, B. Johnson, W. Chen, M. W. Wong, C. Gonzalez and J. A. Pople, *Gaussian 03 (Revision E.01)*, Gaussian, Inc., Wallingford CT, 2004.
31 M. Sućeska, *EXPLO5 6.01*, Brodarski Institute, Zagreb, Croatia, 2013.
32 Test methods according to the UN Manual of Test and Criteria, Recommendations on the Transport of Dangerous Goods, United Nations Publiation, NewYork, Geneva, 4th reviseded, 2003: Impact: Insensitive $\geq$ 40J, less sensitive $\geq$ 35J, sensitive $\geq$ 4J, very sensitive $\geq$ 3J; Friction: Insensitive $>$ 360 N, less sensitive = 360 N, sensitive $<$360 N a. $>$ 80 N, very sensitive $\leq$ 80N, extremely sensitive $\leq$10 N.
33 NATO, Standardization Agreement 4489 (STANAG4489), Explosives, Impact Sensitivity Tests 1999.
34 NATO, Standardization Agreement 4487 (STANAG 4487), Explosives, Friction Sensitivity Tests 2002.
35 M. J. Turner, J. J. M. McKinnon, S. K. Wolff, D. J. Grimwood, P. R. Spackman, D. Jayatilaka and M. A. Spackman, *Crystal Explorer 17*, University of Western Australia, 2017.